HHS Public Access

Author manuscript

Dev Biol. Author manuscript; available in PMC 2017 December 01.

Published in final edited form as:

Dev Biol. 2016 December 1; 420(1): 100–109. doi:10.1016/j.ydbio.2016.10.004.

SHH Ventralizes the Otocyst by Maintaining Basal PKA Activity and Regulating GLI3 Signaling

Sho Ohta[1], **Baolin Wang**[2], **Suzanne L. Mansour**[1,3], and **Gary C. Schoenwolf**[1,*]

[1]Department of Neurobiology and Anatomy, University of Utah School of Medicine, Salt Lake City, Utah

[2]Department of Cell and Developmental Biology, and Genetic Medicine, Weill Cornell Medical College, New York, New York

[3]Department of Human Genetics, University of Utah School of Medicine, Salt Lake City, Utah

Abstract

During development of the inner ear, secreted morphogens act coordinately to establish otocyst dorsoventral polarity. Among these, Sonic hedgehog (SHH) plays a critical role in determining ventral polarity. However, how this extracellular signal is transduced intracellularly to establish ventral polarity is unknown. In this study, we show that cAMP dependent protein kinase A (PKA) is a key intracellular factor mediating SHH signaling through regulation of GLI3 processing. Gain-of-function experiments using targeted gene transfection by sonoporation or electroporation revealed that SHH signaling inactivates PKA, maintaining a basal level of PKA activity in the ventral otocyst. This, in turn, suppresses partial proteolytic processing of GLI3FL, resulting in a low GLI3R/GLI3FL ratio in the ventral otocyst and the expression of ventral-specific genes required for ventral otocyst morphogenesis. Thus, we identify a molecular mechanism that links extracellular and intracellular signaling, determines early ventral polarity of the inner ear, and has implications for understanding the integration of polarity signals in multiple organ rudiments regulated by gradients of signaling molecules.

Keywords

Ventralization; Inner Ear; Otocyst; Polarization; Signaling

Introduction

Morphogen gradients are postulated to provide positional signals that are both sufficient and necessary for establishing the dorsoventral (DV) axis of the otocyst, the primordium of the inner ear (Groves and Fekete, 2012; Wu and Kelley, 2012). Dorsalization of the otocyst involves multiple secreted factors, including WNTs, BMPs, and FGFs (Hatch et al., 2007;

*Correspondence to: Schoenwolf@neuro.utah.edu.

Ohta et al., 2010; Ohta et al., 2016; Ohyama et al., 2006; Riccomagno et al., 2005). In contrast, only one secreted factor, SHH, released from both the floor plate of the neural tube and underlying notochord, has been reported to be required for its ventralization (Riccomagno et al., 2002). *Shh*$^{-/-}$ embryos fail to form cochlear ducts, whereas dorsal inner ear structures still form (Riccomagno et al., 2002). Moreover, factors downstream of SHH also play essential roles in ventral otocyst development. Mice with inactivating mutations in the seven-transmembrane protein, Smoothened, lack cochlear ducts and saccules (Brown and Epstein, 2011). Similarly, mice with C-terminal deletions of GLI3, which express only the repressor form of GLI3, display severely shortened cochlear ducts (Bok et al., 2007). This, and the analysis of other GLI3 mutants in the same study, provides strong evidence that GLI3 activator function is required for normal formation of the cochlear duct.

cAMP-dependent protein kinase A (PKA) plays an important role in regulation of SHH signaling through the posttranslational modification of GLI. In both invertebrate and vertebrate systems, PKA inhibits HH signal transduction (Epstein et al., 1996; Hammerschmidt et al., 1996; Li et al., 2014; Li et al., 1995; Tiecke et al., 2007). In *Drosophila,* genetic and biochemical studies showed that in the absence of HH, activated PKA phosphorylates a cluster of serine residues on the C-terminal domain of cubitus interruptus (Ci), the GLI homolog. This results in the partial proteolysis of Ci to generate a transcriptional repressor form of Ci (Price and Kalderon, 2002). Similarly, in vertebrates, two of the three full-length GLI proteins (GLI2FL and GLI3FL) also undergo PKA-dependent phosphorylation and partial proteolytic processing to generate a repressor form (GLIR), with GLI3R being the most prominent (Pan and Wang, 2007; Wang et al., 2000).

Activation of PKA plays a crucial role in polarization of the vertebrate neural tube. Blocking PKA activity in zebrafish embryos ventralizes the neural tube, as shown by dorsal expansion of the ventral marker gene, *axial* (Epstein et al., 1996; Hammerschmidt et al., 1996). Similarly, in PKA-deficient mouse embryos, the number of SHH-dependent ventral cell types in the developing neural tube is expanded (Tuson et al., 2011). These findings suggest that PKA acts in DV polarization of the neural tube by negatively regulating SHH signaling.

Here, we used western blotting and gene mis-expression to reveal roles for SHH signaling and PKA in establishing the DV axis of the otocyst. We show that PKA forms a DV gradient of activity across both the chick and mouse otocyst, being low ventrally and high dorsally, which parallels a DV gradient in GLI3 protein processing to establish a DV gradient of the ratio of GLI3R to GLI3FL. Overexpression of SHH inhibits PKA and pCREB labeling in the chick dorsal otocyst and alters dorsal gene expression, blocking formation of the semicircular canals. Finally, inhibition of PKA in the chick otocyst with the PKA inhibitor alpha (PKIα), or overexpression of GLI3A, also ventralizes the otocyst. Thus, SHH signaling through inhibition of PKA plays an important role in establishing the ventral patterning of the otocyst.

Material and methods

Embryos

Fertilized White Leghorn chicken eggs were purchased from Merrill's Poultry Farm (Paul, Idaho, USA). Eggs were incubated at 38.5°C and staged according to the criteria of Hamburger and Hamilton (HH; (Hamburger and Hamilton, 1951). CD-1 (Charles River) mouse embryos were collected on the indicated days following detection of a mating plug. The use of mice complied with a University of Utah approved IACUC protocol.

PKA activity assay

Dissected otocysts (chick: HH stages 20-24; mouse: E10.5-11.0), either kept intact or dissected into dorsal (do), middle (mi), and ventral (ve) fragments, were pooled (5-20 for each lane), enzymatically digested with dispase (GIBCO: working concentration of 0.5 U/ml for 30-45 min at 37°C), and lysed in buffer consisting of 25mM Tris-HCl (pH 7.4), 0.5 mM EDTA, 0.5mM EGTA, and 10 mM β-mercaptoethanol, with one inhibitor cocktail tablet (Complete, Roche #1836153) added per 50 ml. PKA activity was measured using a commercially available kit (PepTag Non-radioactive detection of cAMP-dependent protein kinase assay system, Promega, #V5340), according to the manufacturer's instructions.

pCREB staining and quantification of signal intensity

We detected pCREB in tissue sections by using a phospho-specific primary antibody (rabbit polyclonal, MILLIPORE, cat. # 06-519) diluted 1:1000 in blocking solution (0.1% FBS). A Vectastain ABC HRP kit (cat# PK-4001) was used according to the manufacturer's manual for enhancing the signal with HRP visualized with 3,3′-diaminobenzidine (DAB, SIGMA, cat# D5905).

To quantify pCREB signal intensity in tissue sections, we used an ImageJ macro, kindly developed by Dr. H. Otsuna, VoxelPress (https://dl.dropboxusercontent.com/u/4774326/VoxelPress/Products.html). The signal to noise (background) labeling of pCREB was variable from embryo to embryo, even in groups of the same type of embryo at the same stage and processed identically in the same batch. Hence, to ensure that accurate measurements of pCREB labeling could be made independently of observer bias, we used the macro to automatically normalize the signal intensity of pCREB labeling in the wall of the otocyst in multiple sections through approximately its mid-craniocaudal extent. To detect regional differences in control otocysts (dorsolateral, ventromedial, etc.) at different stages, or in otocysts from embryos into which *Shh* was sonoporated, masks were manually created in ImageJ to segment the analysis. To compare electroporated (i.e., GFP-positive) cells in control and experimental otocysts, the macro automatically created masks to restrict the analysis to fluorescent cells.

In ovo gene transduction

Chick eggs were windowed using standard techniques, and embryos at HH stages 15-16 were either sonoporated (Ohta et al., 2003) or electroporated (Ohta et al., 2010) *in ovo* to transfect expression vectors. For sonoporation, a DNA-microbubble mixture was prepared by adding 10 μl of a plasmid DNA solution (concentration 2.0-4.0 μg/μl), consisting of

pCAGGS-*Gfp* alone or pCAGGS-*Gfp* and pCAGGS-c*Shh* to 10 μl of SonoVue (BRACCO, Protech, Texas, USA), a microbubble solution used for gene transfection. The DNA-microbubble mixture was then injected into the head mesenchyme adjacent to the developing otocyst using a glass micropipette (GD-1.2: Narishige, Tokyo, Japan). Injected embryos were immediately exposed to ultrasound using a 3-mm diameter ultrasound probe (Sonitron 2000N, Nepagene, Japan) with an input frequency of 1 MHz, an output intensity of 2.0 W/cm^2, and a pulse duty ratio of 20% for a duration of 60 seconds.

For electroporation, the plasmid solution contained 0.1% fast green to enable visualization of the injection site and consisted of either 2.0 μg/μl of pCAGGS-*Gfp* alone or 2.0 μg/μl of pCAGGS-*Gfp* and pCAGGS-h*Pkia* or 2.0 μg/μl of pCAGGS-h*Gli3A*^{HIGH}. DNA was injected into the lumen of the developing otocyst using a fine glass micropipette with positive and negative electrodes positioned accordingly. Two 50-msec pulses at 10 volts were then applied using a CUY21 electroporator. Because the wall of the otocyst was impaled with an electrode during electroporation, localized damage of the wall was sometimes detected, with a small cluster of dying cells present in the lumen. However, the damaged region and dying cells were excluded from our subsequent analyses.

Transfected cells were identified in tissue sections by using an antibody directed against GFP (mouse monoclonal, Roche, #11814460001). AlexaFluor 488-labeled donkey anti-mouse IgG (Invitrogen, cat. #A21202), diluted 1:1000, was used as the secondary antibody.

Expression vectors

pCAGGS-*Gfp* was kindly provided by Dr. H. Ogawa (Ogawa et al., 1995) and pCAGGS-*Gli3A*^{HIGH} by Dr. J. Briscoe (Persson et al., 2002; Stamataki et al., 2005). pCAGGS-c*Shh* was described previously (Ohta et al., 2010; Ohta et al., 2003). Full-length human cDNA encoding protein kinase inhibitor alpha (h*Pkia*) was purchased from DNAFORM (cDNA clone ID: 4288676, http://www.dnaform.jp/) and inserted into a pCAGGS vector.

Three-dimensional (3D) reconstruction of the inner ear

To visualize the 3-D structure of the chick inner ear, paraffin serial transverse sections of chick embryos at HH stage 30 were stained with hematoxylin and eosin. Sections were then photographed, and control and experimental inner ears were reconstructed using Amira 5.1 software (FEI Company, FEI.com).

In situ hybridization on paraffin sections

Chick and mouse embryos were fixed with 4% paraformaldehyde and embedded in paraffin, and transverse sections were subjected to *in situ* hybridization (ISH) using standard procedures with chick (c) probes for c*Pax2, cOtx2, cNkx5.1,* and *cDlx5* (kindly provided, respectively, by Drs. D. Henrique, L. Bally-Cuif, E. Bober, W. Upholt). *cPax2* was used to mark the ventromedial otocyst (Sanchez-Calderon et al., 2005); *cOtx2,* the ventrolateral otocyst (Morsli et al., 1999); and *cNkx5.1* and *cDlx5,* the dorsolateral otocyst (Brown et al., 2005; Hadrys et al., 1998).

Western blotting

For western blotting, otocysts were manually dissected from embryos digested with dispase at desired stages (chick: HH stages 20-24; mouse: E10.5-11.0), either kept intact or dissected into dorsal (do), middle (mi), and ventral (ve) fragments, pooled (5-20 for each lane), and lysed with ice-cold RIPA buffer. Protein concentration was measured using the Bradford assay (Coomassie Plus Protein Assay Reagent, cat. #1856210, Thermo Science). Equal amounts of protein were loaded onto 7.5% SDS-PAGE gels, and western blotting was performed with GLI3 or GLI2 antibody as described previously (Pan and Wang, 2007; Wang et al., 2000). An antibody to α-tubulin (1:2000, Sigma, #T6199) was used as loading control.

Statistical analysis

Statistical analyses were performed using Minitab Express (Minitab). In each experiment, we used the Anderson-Darling test to evaluate whether the data fit a normal distribution, and the F-test to examine whether variances between the two groups (control and experimental) were similar. Based on this, means and standard derivations were calculated and shown in the graphs, with *P*-values obtained using a two-tailed, unpaired Student's t-test.

Results

PKA activity is graded across the otocyst DV axis

The ventral otocyst, as compared with the dorsal otocyst, likely receives a high concentration of SHH, as it develops in close proximity to the source of SHH secretion from the floor plate and notochord. Consistent with this, the expression of *Patched1* and *Gli1* mRNA, transcriptional readouts of SHH signaling, are detected in a gradient pattern with a high level in the ventromedial otocyst and a low level in the dorsolateral otocyst (Bok et al., 2007; Brown and Epstein, 2011). The binding of SHH ligands to the Patched1 receptor is thought to block the inhibition of Smoothened by Patched and inactivate PKA (Ayers and Therond, 2010; Milenkovic and Scott, 2010), leading to the prediction that PKA activity is lower in the ventromedial otocyst than in the dorsolateral otocyst, thus resulting in a dorsal-high to ventral-low gradient across the otocyst.

To measure PKA activity, we removed otocysts from chick and mouse embryos, subdivided each into dorsal (D), middle (M), and ventral (V) fragments (Fig. 1A, A'), and measured PKA activity in pooled fragments. A statistically significant DV gradient of PKA activity occurred across both chick and mouse otocysts, with low activity ventrally and high activity dorsally (Fig. 1B, B'). In addition to analyzing the spatial and temporal distribution of PKA activity in the otocyst, we examined phosphorylation of cAMP response element binding (CREB) protein, a substrate of PKA (Shaywitz and Greenberg, 1999). In chick otocysts as early as at HH stage 16, a stage at which the dorsal rim of the otic cup had just closed, and in mouse otocysts as early at E9.0, a statistically significant dorsal-high to ventral-low gradient of pCREB labeling was present, which persisted during later stages (Fig. 1C, C'). Collectively, these results show that graded PKA activity occurs across the DV axis of the otocyst during the earliest stages of inner ear development when DV patterning is being established.

SHH inhibits PKA activity and induces ventral polarity of the otocyst

To determine whether SHH affects PKA activity, we overexpressed SHH by sonoporating a *Shh*-expression vector into the dorsal head mesenchyme of chick embryos at HH stages 15-16 (Fig. 2A, 2A') and incubating eggs until desired stages were reached. Control otocysts were obtained from the non-sonoporated (left) side.

To measure PKA activity, embryos were incubated an additional 12 or 24 hours after sonoporation, and otocysts were removed. In comparison with control otocysts, PKA activity was significantly reduced in SHH-treated otocysts (Fig. 2B). Similarly, in the dorsal otocyst, where robust pCREB labeling occurred in control otocysts, pCREB labeling was significantly reduced 12 hours after *Shh* overexpression, and even more so by 24 hours (Fig. 2C). These results show that SHH can inhibit PKA activity in the otocyst during inner ear development, and that this regulation occurs relatively quickly after SHH transfection.

Next, we asked whether SHH affects DV development of the early otocyst. Overexpression of *Shh* resulted in a complete loss of the three semicircular canals 5-6 days later, whereas the cochlear duct formed normally (Fig. 2D). Thus, dorsal development of the otocyst was inhibited by overexpression of *Shh*. To ask whether gene expression was altered in the dorsal otocyst prior to the loss of the semicircular canals, we analyzed by ISH genes that are regionally expressed within the otocyst at HH stages 24-25. After *Shh* overexpression, *Pax2*, a gene normally expressed in the ventromedial region of otocyst, was also expressed ectopically in the dorsolateral otocyst (Fig. 2E, E'). *Otx2*, a gene normally expressed ventrally in the otocyst in the nascent cochlear duct, now expanded its expression into the dorsolateral otocyst (Fig. 2F, F'). *Hmx3*, a gene normally restricted mainly to the dorsal otocyst, showed virtually no expression (Fig. 2G, G'). In contrast, expression of *Dlx5*, a gene normally expressed mainly in the dorsolateral otocyst, was unchanged (Fig. 2H H'). Collectively, these results suggest that SHH signaling acts during normal development of the otocyst to induce ventral polarity, which ultimately results in the failure of dorsal morphogenesis.

We noticed one other change in the otocyst after *Shh* overexpression. The endolymphatic duct was hypertrophied (Fig. 2C, asterisk) and, subsequently, cells seemed to be dying, as suggested by the presence of rounded cells in the duct and in the otocyst lumen; Figs. 2E', F', G'). In earlier studies, we did not detect these changes after overexpression of *Bmp* by sonoporation (Ohta et al., 2010; Ohta et al., 2016); however, sonoporation of *Noggin*, a BMP inhibitor, had an effect on the endolymphatic duct similar to that of *Shh* (Ohta et al., 2016: Fig. 2F). These results raise the possibility that BMP is a survival factor for the endolymphatic duct and further suggests that sonoporation per se is not deleterious for development of the otocyst or endolymphatic duct.

Decreasing PKA activity, like overexpression of *Shh*, induces ventral polarity of the otocyst

The experiments just described suggest that overexpression of SHH signaling ventralizes the otocyst and is accompanied by decreased PKA activity. Thus, we next asked whether decreased PKA activity also ventralizes the otocyst. To do this, we either co-electroporated

Pkia and *Gfp* vectors or electroporated *Gfp* vector alone into the epithelium of the dorsal otocyst (Fig. 3A, A'). PKI functions contains a pseudo-substrate sequence that inhibits PKA enzymatic activity by binding to and inhibiting the activity of the catalytic subunit of PKA (Scott et al., 1985) or by triggering exit of the PKI/PKA complex from the nucleus. In addition, *Pkia* also contains a nuclear export signal (Wen et al., 1994; Wen et al., 1995). Binding of PKI to the catalytic subunit of PKA exposes the nuclear export signal, triggering exit of the complex from the nucleus. Twelve hours after electroporation, we examined PKA activity in the transfected cells using pCREB labeling. This showed that a significant decrease in pCREB labeling occurred in the cells transfected with *Pkia* and *Gfp* vectors, as compared with those transfected with *Gfp* vector alone (Fig. 3B).

To determine whether the dorsal-high level of PKA activity in the otocyst is required for development of dorsal structures, we examined the developing inner ear 5-6 days after attenuating PKA activity by overexpressing *Pkia*. This showed that loss of PKA activity in the dorsal otocyst blocked formation of the three semicircular canals, although a primordial canal pouch still developed, whereas the cochlear duct formed normally (Fig. 3C). Thus, otocysts subjected either to gain of SHH signaling or reduction of PKA activity showed blocked dorsal development, but the resulting phenotypes differed dramatically.

Next, we asked whether decreasing PKA activity in the dorsal otocyst induced ventral polarity, as did overexpression of *Shh*. Otocysts were again either co-electroporated with *Pkia* and *Gfp* vectors or electroporated with *Gfp* vector alone and examined with ISH 18-24 hours later. *Pax2* was ectopically expressed in the dorsal otocyst in cells that were also positive for GFP; that is, cells presumably also transfected with *Pkia* (Fig. 3D, D'). In addition, both the dorsal boundary of the *Otx2*-expression domain (arrowhead, Fig. 3E, E') and the ventral boundary of the *Hmx3*-expression domain (Fig. 3F, F') shifted dorsally after *Pkia* overexpression, and the expression *Hmx3* was almost abolished in transfected cells. Collectively, these results suggest that decreasing PKA activity in the dorsal otocyst ventralizes the otocyst—in other words, that high-PKA activity is required to establish the dorsal polarity of the developing inner ear. Moreover, the dorsal shift in the boundary between the *Hmx3*- and *Otx2*-expression domains provides further evidence that a dorsal-high to ventral-low PKA gradient is present in the otocyst and is functionally relevant for inner ear patterning.

As mentioned above, dramatically different phenotypes resulted in the dorsal otocyst after overexpression of *Shh* and *Pkia* (cf., Figs. 2D, 3C). The most likely explanation of this difference is a technical one: *Shh* overexpressed by sonoporation acted on virtually all of the cells in the dorsolateral otocyst, whereas *Pkia* overexpressed by electroporation acted on a much smaller subset of cells. This is supported by the observation that expression *Hmx3* of was essentially extinguished after *Shh* overexpression but not after *Pkia* (cf., Figs. 2G', 3F').

A dorsal-high to ventral-low gradient of the ratio of GLI3 repressor to GLI3 full-length forms across both chick and mouse otocysts, and decreasing PKA activity dorsally decreases the GLI3R level

Our results so far beg the question of why the otocyst is ventralized by decreasing PKA activity dorsally. Previous studies showed that PKA phosphorylates GLI3 full-length protein (GLI3FL), a process required for posttranslational modification through partial proteolytic processing to form GLI3 repressor (GLI3R) (Pan and Wang, 2007; Wang et al., 2000). Thus, we postulated that in the untreated otocyst, the dorsal region, which has higher PKA activity, would have greater GLI3FL processing than the ventral otocyst, which has lower PKA activity and would have less GLI3FL processing.

To ascertain whether GLI3FL processing is higher dorsally, we examined the distribution of GLI3FL and GLI3R across the DV axis of the otocyst by western blotting. As described above, dorsal, middle, and ventral otocyst fragments were collected from HH stage 24 chick and E10.5-E11.0 mouse otocysts and pooled for protein extraction. Both GLI3R and GLI3FL were clearly distributed in a dorsal-high to ventral-low gradient in the chick otocyst (Fig. 4A). However, in the mouse otocyst, only GLI3R was distributed in this manner, with GLI3FL being distibuted uniformly across the DV axis of the otocyst (Fig. 4B). Nevertheless, in both species, the ratio of GLI3R to GLI3FL formed a statistically significant dorsal-high to ventral-low gradient (Figs. 4A, B: graphs). This result is consistent with the prediction made previously by analyzing GLI mutant mouse embryos (Bok et al., 2007). We also considered whether GLI2, which is the only other GLI family member thought to be proteolytically processed like GLI3 from a full-length form to a repressor form, distributes in a gradient similar to that of GLI3. Because the GLI2 antibody did not recognize chick GLI2, we were able to obtain western blotting data only for mouse otocysts. Unlike GLI3, concentration gradients of GLI2R or GLI2FL were not observed, and the ratio of GLI2R to GLI2FL was not statistically changed across the DV axis of the otocyst (Fig. 4C).

Next, we asked whether proteolytic processing of GLI3FL in the otocyst depends on PKA activity. To do this, we again transfected otocysts dorsally with *Pkia* (Fig. 4D) and collected otocysts 24 hours later for western blotting; the non-electroporated otocyst served as a control. The ratio of GLI3R to GLI3FL decreased significantly after *Pkia* transfection due to a reduction in the amount of GLI3R, suggesting that high PKA activity ventrally is required to establish the high GLI3R/GLI3FL ratio across the otocyst.

A low GLI3R to GLI3FL ratio is required ventrally to establish ventral otocyst polarity

The results of our experiments described so far indicate that low PKA activity results in minimal GLI3FL proteolytical processing, which in turn results in ventralization in the otocyst. Therefore, we next asked whether low GLI3FL processing, which results in a high level of GLI3FL (potentially GLI3A), is sufficient to induce ventral polarity. To do this, we overexpressed a constitutively active *Gli3A, Gli3A*^{HIGH}, in the dorsal otocyst by electroporation (Fig. 3A), counteracting the high level of GLI3R normally present there (the non-electroporated otocyst served as a control). In developing inner ears examined 5-6 days after *Gli3A* overexpression, all three semicircular canals were completely absent, although

the primordial canal pouch still formed, whereas the cochlear duct was normal (Fig. 5A). This phenotype was strikingly similar to that occurring after *Pkiα* overexpression (cf., Figs. 3C and 5A).

Gene expression was then analyzed in both *Gli3A/Gfp* (experimental) and *Gfp* (control) otocysts at HH stages 20-21. Ectopic *Pax2* expression occurred in *Gli3A*-transfected cells in the dorsal otocyst (Fig. 5B). However unlike *Pax2*, *Otx2* expression was not induced in *Gli3A*-transfected cells (Fig. 5C). In contrast to *Pax2* and *Otx2*, *Hmx3* expression was decreased in dorsal *Gli3A*-transfected cells (Fig. 5D), whereas the *Dlx5*, another dorsally expressed otocyst gene, was unaffected (Fig. 5E). Collectively, these results show that GLI3A is sufficient to establish the ventral polarity of the otocyst.

Discussion

It has been known for over a decade that SHH signaling plays a central role in ventral patterning of the otocyst (Bok et al., 2005; Riccomagno et al., 2002), but how SHH signaling is transduced intracellularly was unknown. We show here that dorsal-high to ventral-low gradients of both PKA activity and the ratio of GLI3R to GLI3FL occur in the early otocyst, and that SHH signaling maintains low PKA activity and a low GLI3R/GLI3FL ratio in the ventral otocyst. This, in turn, results in the expression of genes required for ventral otocyst patterning and cochlear morphogenesis (Fig. 6).

The PKA activity gradient across the DV axis of the otocyst is established by signaling from extracellular secreted proteins

In this study we showed that increasing SHH signaling in the dorsal otocyst decreases the high level of PKA activity normally there, and decreases CREB phosphorylation. This suggests that SHH signaling from the notochord and the floor plate of the neural tube negatively regulates the activation of PKA, in support of the results from studies of cerebellum and retina (Barzi et al., 2010; Trousse et al., 2001). Because PKA activation is controlled by the intracellular level of cAMP, inhibition of PKA activity by SHH signaling is thought to involve a reduction in the level of intracellular cAMP (Murray, 2008). Retinal ganglion axons treated with SHH strikingly reduce their intracellular cAMP level (Trousse et al., 2001). Moreover, studies in both invertebrate and vertebrate embryos show that HH signaling antagonizes the cAMP/PKA pathway. In *Drosophila*, Smoothened, a member of the G-protein-coupled receptor (GPCR) family, activates Gαi when HH ligands are present, resulting in inhibition of adenylate cyclase, and, consequently, reduction of intracellular cAMP levels (Ayers and Therond, 2010); this, in turn, blocks activation of PKA.

In the vertebrate neural tube, as SHH ligand binds to its receptor Patched, Smoothened is activated (Rohatgi and Scott, 2007) and Gpr161, likely to be $G\alpha_s$ coupled, is internalized and transported out of the cilium, reducing the level of cAMP (Mukhopadhyay et al., 2013). The reduction of cAMP attenuates PKA activity. Our results presented here show that SHH signaling also downregulates PKA activity in the ventral region of the developing inner ear, but further study is needed to determine whether is does so in the same manner as in the neural tube or through another mechanism.

In contrast to the ventral region of the otocyst, its dorsal region normally has high PKA activity and high pCREB labeling. We think that this is due not only to the fact that the dorsal region of otocyst is farther from the source of SHH signaling, but also that secreted molecules such as BMP and WNT act on the dorsal otocyst to increase PKA activity. Our recent study showed that BMP signaling upregulates PKA activity (Ohta et al., 2016), suggesting that BMPs secreted from the roof plate of the neural tube or the nascent cristae of the otocyst likely play an essential role in regulating the high dorsal level of PKA activity. WNT signaling may also participate in establishing high PKA activity in the dorsal otocyst, as WNT signaling is known to activate the PKA/CREB pathway during somitic myogenesis (Chen et al., 2005). Taken together, graded PKA activity across the DV axis of the otocyst is precisely regulated by secreted molecules including SHH, BMPs, and WNTs.

The dorsal-high to ventral-low gradient of PKA activity establishes the dorsal-high to ventral-low gradient of GLI3R/GLI3FL

The study of various alleles of GLI mutant mice led to the prediction that reciprocal gradients of GLI repressor and activator across the DV axis of the otocyst are responsible for the specification of the dorsal and the ventral structure of the inner ear (Bok et al., 2007). Using western blotting, we show here that dorsal-high to ventral low gradients in the ratio of GLI3R to GLI3FL form across the DV axis of both chick and mouse otocysts. Thus, our results support the previous prediction by showing that GLI3R activity predominates dorsally and GLI3FL (GLI3A) activity predominates ventrally. Furthermore, we show that the gradient in the ratio of GLI3R/GLI3FL is required to establish DV patterning of the early otocyst through the regulation of regionally expressed otocyst genes, which drive vestibular and cochlear duct development. The ratio of GLI3R to GLI3FL proteins is largely established by differences in the processing of GLI3FL across the DV axis of the otocyst. PKA is required for the initial phosphorylation of GLI3FL, which results in its posttranslational proteolytic processing to GLI3R (Wang et al., 2000). Considering the importance of PKA in GLI3FL processing, a dorsal-high to ventral-low gradient of PKA likely accounts for the gradient in GLI3FL processing; that is, the dorsal otocyst has high PKA activity, which correlates with high GLI3FL processing, whereas the ventral otocyst has low PKA activity, which correlates with low GLI3 processing.

We showed previously that GLI3FL processing in the otocyst was increased after overexpression of ca*Pka* ventrally, resulting in an increased GLI3R/GLI3FL ratio (Ohta et al., 2016), and in the current study that overexpression of *Pkia* dorsally resulted in a decreased GLI3R/GLI3FL ratio. Collectively, these results support the idea that processing of GLI3FL to GLI3R during development of the otocyst depends at least partially on PKA activity. Although our results provide strong evidence that PKA acts in the processing of GLI3FL to GLI3R in the chick otocyst, whether this occurs universally during development of vertebrates is controversial. For example, during development of the chick limb bud, the source of SHH signaling (the ZPA) is localized posteriorly, and, correspondingly, the level of GLI3FL is high posteriorly and that of GLI3R is high anteriorly (Wang et al., 2000). But PKA activity is high in the posterior limb bud and low in the anterior limb bud (the opposite would be expected if PKA causes GLI3FL processing in the limb bud) (Tiecke et al., 2007). Furthermore, in mouse embryos lacking PKA, GLI3R is still present, although the total

amount of GLI3 protein is reduced (Tuson et al., 2011). Further studies are needed to resolve the discrepant results among the different studies, which may reflect other events such as compensation by other protein kinases.

SHH signaling positively regulates expression of ventral regional genes and simultaneously suppresses the expression of dorsal regional genes

It has been known for over a decade that SHH signaling is essential for establishing the ventral polarity of the early otocyst and the subsequent outgrowth of the cochlear duct (Riccomagno et al., 2002). In addition to the traditional SHH signaling sources, the floor plate of neural tube and the notochord, the developing cochleovestibular ganglion provides another SHH signaling source that acts in cochlear duct extension (Bok et al., 2013; Ohyama et al., 2006; Riccomagno et al., 2002). Loss of SHH signaling results in the loss or reduction of ventral gene expression and the absence of ventral otocyst development (Brown and Epstein, 2011; Riccomagno et al., 2002). Among the ventral regional genes that are perturbed in the SHH null mutant, *Pax2, Otx1* and *Otx2* seem to be essential for formation of the cochlear duct (Riccomagno et al., 2002). *Pax2* is normally expressed in the ventromedial otocyst and in the *Pax2* null mutant mouse apoptosis occurs ventrally, resulting in truncation of the cochlear duct (Burton et al., 2004). *Otx1* and *Otx2*, unlike *Pax2*, are expressed in the ventrolateral otocyst (Morsli et al., 1999). Consistent with these expression patterns, $Otx1^{-/-}$; $Otx2^{+/-}$ mice lack the lateral semicircular canal and have a shortened cochlear duct (Morsli et al., 1999). Conversely, overexpression of SHH or *Pkia* in the current study resulted in ectopic expression of *Pax2* and expansion of the *Otx2* expression domain in the dorsal otocyst. Collectively, these results suggest that SHH signaling positively regulates the expression of both *Pax2* and *Otx* genes, but it is likely that SHH signaling regulates the expression of these genes in a different manner. After overexpression of *Gli3A* in the dorsal otocyst, *Pax2* expression, but not *Otx2* expression, occurs ectopically in *Gli3A*-transfected cells. Thus, *Pax2* is a target of SHH/GLI3A signaling but *Otx2* is not. However, *Gli3R* overexpression in the ventral otocyst inhibited *Otx2* expression (Ohta et al., 2016). Thus, *Otx2* expression likely occurs in the ventral otocyst because the level of GLI3R is low owing to strong SHH signaling in this region, allowing its expression to be promoted by other unknown transcription factors. Why, then, does the overexpression of *Gli3A* and *Pkia* have different effects on *Otx2* expression in our experiments? *Gli3A* overexpression would be expected to increase the level of GLI3A in transfected cells but a high level of GLI3R, which inhibits *Otx2* expression, would remain. In contrast, *Pkia* overexpression would decrease the level of GLI3R, allowing for *Otx2* expression.

SHH signaling is also believed to determine the ventral polarity of the otocyst by antagonizing the expression of dorsal regional genes in the ventral otocyst. *ShhP1* transgenic mice carrying a SHH transgene that is ectopically expressed in the dorsal otocyst have decreased otocyst expression of both *Dlx5* and *Hmx3* (Riccomagno et al., 2002), both of which are required to form the dorsal structures of the inner ear (Hadrys et al., 1998; Merlo et al., 2002; Wang et al., 2004; Wang et al., 1998). In our current study, overexpression of *Shh* in the dorsal otocyst also resulted in a dramatic reduction in *Hmx3* expression in the dorsal otocyst, but *Dlx5* expression was unchanged. Furthermore, overexpression of *Gli3A* in the dorsal otocyst suppressed *Hmx3*, but not *Dlx5* expression. These data indicate that

SHH signaling via GLI3A negatively regulates expression of *Hmx3* to determine ventral polarity. In contrast to *Hmx3*, we showed recently that *Dlx5* expression in the dorsal otocyst is regulated positively by the BMP-pSMAD pathway (Ohta et al., 2016).

Conclusions

In this study, we present a new model (Fig. 6) for establishing the ventral polarity of the early otocyst in which SHH, emanating from the floor plate of the neural tube and the notochord, decreases PKA activity, thereby reducing the proteolytic processing of GLI3FL and regulating the expression of ventral regional genes. We showed previously that BMP signaling in the dorsal otocyst activates PKA and, in turn, increases GLI3 processing to from GLI3 repressor, so that a dorsal-high to ventral-low gradient of the ratio of GLI3 repressor to GLI3 activator forms (Ohta et al., 2016). The GLI3R/GLI3FL ratio regulates the expression of regional genes, *Pax2*, *Otx2,* and *Hmx3*, but not that of *Dlx5*, and is thus responsible for the specification of the regional identity and the structural components of the inner ear along the DV axis. We conclude that regulation of PKA activity provides a common point for integrating dorsal and ventral polarity signals.

Acknowledgments

We thank Yukio Saijoh and Lisa Urness for critical comments. The research reported herein was supported by the National Institute on Deafness and Other Communication Disorders of the National Institutes of Health (R01 DC011819 to S.L.M. and G.C.S.) and the National Institute of General Medical Sciences of the National Institutes of Health (R01 GM114429 to B.W.). The content is solely the responsibility of the authors and does not necessarily represent the official views of the National Institutes of Health.

References

Ayers KL, Therond PP. Evaluating Smoothened as a G-protein-coupled receptor for Hedgehog signalling. Trends Cell Biol. 2010; 20:287–298. [PubMed: 20207148]

Barzi M, Berenguer J, Menendez A, Alvarez-Rodriguez R, Pons S. Sonic-hedgehog-mediated proliferation requires the localization of PKA to the cilium base. J Cell Sci. 2010; 123:62–69. [PubMed: 20016067]

Bok J, Bronner-Fraser M, Wu DK. Role of the hindbrain in dorsoventral but not anteroposterior axial specification of the inner ear. Development. 2005; 132:2115–2124. [PubMed: 15788455]

Bok J, Dolson DK, Hill P, Ruther U, Epstein DJ, Wu DK. Opposing gradients of Gli repressor and activators mediate Shh signaling along the dorsoventral axis of the inner ear. Development. 2007; 134:1713–1722. [PubMed: 17395647]

Bok J, Zenczak C, Hwang CH, Wu DK. Auditory ganglion source of Sonic hedgehog regulates timing of cell cycle exit and differentiation of mammalian cochlear hair cells. Proc Natl Acad Sci U S A. 2013; 110:13869–13874. [PubMed: 23918393]

Brown AS, Epstein DJ. Otic ablation of smoothened reveals direct and indirect requirements for Hedgehog signaling in inner ear development. Development. 2011; 138:3967–3976. [PubMed: 21831920]

Brown ST, Wang J, Groves AK. Dlx gene expression during chick inner ear development. J Comp Neurol. 2005; 483:48–65. [PubMed: 15672396]

Burton Q, Cole LK, Mulheisen M, Chang W, Wu DK. The role of Pax2 in mouse inner ear development. Dev Biol. 2004; 272:161–175. [PubMed: 15242798]

Chen AE, Ginty DD, Fan CM. Protein kinase A signalling via CREB controls myogenesis induced by Wnt proteins. Nature. 2005; 433:317–322. [PubMed: 15568017]

Epstein DJ, Marti E, Scott MP, McMahon AP. Antagonizing cAMP-dependent protein kinase A in the dorsal CNS activates a conserved Sonic hedgehog signaling pathway. Development. 1996; 122:2885–2894. [PubMed: 8787761]

Groves AK, Fekete DM. Shaping sound in space: the regulation of inner ear patterning. Development. 2012; 139:245–257. [PubMed: 22186725]

Hadrys T, Braun T, Rinkwitz-Brandt S, Arnold HH, Bober E. Nkx5-1 controls semicircular canal formation in the mouse inner ear. Development. 1998; 125:33–39. [PubMed: 9389661]

Hamburger V, Hamilton HL. A series of normal stages in the development of the chick embryo . J Morphol. 1951; 88:49–92. [PubMed: 24539719]

Hammerschmidt M, Bitgood MJ, McMahon AP. Protein kinase A is a common negative regulator of Hedgehog signaling in the vertebrate embryo. Genes Dev. 1996; 10:647–658. [PubMed: 8598293]

Hatch EP, Noyes CA, Wang X, Wright TJ, Mansour SL. Fgf3 is required for dorsal patterning and morphogenesis of the inner ear epithelium. Development. 2007; 134:3615–3625. [PubMed: 17855431]

Li S, Ma G, Wang B, Jiang J. Hedgehog induces formation of PKA-Smoothened complexes to promote Smoothened phosphorylation and pathway activation. Sci Signal. 2014; 7:ra62. [PubMed: 24985345]

Li W, Ohlmeyer JT, Lane ME, Kalderon D. Function of protein kinase A in hedgehog signal transduction and Drosophila imaginal disc development. Cell. 1995; 80:553–562. [PubMed: 7867063]

Merlo GR, Paleari L, Mantero S, Zerega B, Adamska M, Rinkwitz S, Bober E, Levi G. The Dlx5 homeobox gene is essential for vestibular morphogenesis in the mouse embryo through a BMP4-mediated pathway. Dev Biol. 2002; 248:157–169. [PubMed: 12142028]

Milenkovic L, Scott MP. Not lost in space: trafficking in the hedgehog signaling pathway. Sci Signal. 2010; 3:pe14. [PubMed: 20388915]

Morsli H, Tuorto F, Choo D, Postiglione MP, Simeone A, Wu DK. Otx1 and Otx2 activities are required for the normal development of the mouse inner ear. Development. 1999; 126:2335–2343. [PubMed: 10225993]

Mukhopadhyay S, Wen X, Ratti N, Loktev A, Rangell L, Scales SJ, Jackson PK. The ciliary G-protein-coupled receptor Gpr161 negatively regulates the Sonic hedgehog pathway via cAMP signaling. Cell. 2013; 152:210–223. [PubMed: 23332756]

Murray AJ. Pharmacological PKA inhibition: all may not be what it seems. Sci Signal. 2008; 1:re4. [PubMed: 18523239]

Ogawa H, Inouye S, Tsuji FI, Yasuda K, Umesono K. Localization, trafficking, and temperature-dependence of the Aequorea green fluorescent protein in cultured vertebrate cells. Proc Natl Acad Sci U S A. 1995; 92:11899–11903. [PubMed: 8524871]

Ohta S, Mansour SL, Schoenwolf GC. BMP/SMAD signaling regulates the cell behaviors that drive the initial dorsal-specific regional morphogenesis of the otocyst. Dev Biol. 2010; 347:369–381. [PubMed: 20837004]

Ohta S, Suzuki K, Tachibana K, Yamada G. Microbubble-enhanced sonoporation: efficient gene transduction technique for chick embryos. Genesis. 2003; 37:91–101. [PubMed: 14595845]

Ohta S, Wang B, Mansour SL, Schoenwolf GC. BMP regulates regional gene expression in the dorsal otocyst through canonical and non-canonical intracellular pathways. Development. 2016; 143:2228–2237. [PubMed: 27151948]

Ohyama T, Mohamed OA, Taketo MM, Dufort D, Groves AK. Wnt signals mediate a fate decision between otic placode and epidermis. Development. 2006; 133:865–875. [PubMed: 16452098]

Pan Y, Wang B. A novel protein-processing domain in Gli2 and Gli3 differentially blocks complete protein degradation by the proteasome. J Biol Chem. 2007; 282:10846–10852. [PubMed: 17283082]

Persson M, Stamataki D, te Welscher P, Andersson E, Bose J, Ruther U, Ericson J, Briscoe J. Dorsal-ventral patterning of the spinal cord requires Gli3 transcriptional repressor activity. Genes Dev. 2002; 16:2865–2878. [PubMed: 12435629]

Price MA, Kalderon D. Proteolysis of the Hedgehog signaling effector Cubitus interruptus requires phosphorylation by Glycogen Synthase Kinase 3 and Casein Kinase 1. Cell. 2002; 108:823–835. [PubMed: 11955435]

Riccomagno MM, Martinu L, Mulheisen M, Wu DK, Epstein DJ. Specification of the mammalian cochlea is dependent on Sonic hedgehog. Genes Dev. 2002; 16:2365–2378. [PubMed: 12231626]

Riccomagno MM, Takada S, Epstein DJ. Wnt-dependent regulation of inner ear morphogenesis is balanced by the opposing and supporting roles of Shh. Genes Dev. 2005; 19:1612–1623. [PubMed: 15961523]

Rohatgi R, Scott MP. Patching the gaps in Hedgehog signalling. Nature cell biology. 2007; 9:1005–1009. [PubMed: 17762891]

Sanchez-Calderon H, Martin-Partido G, Hidalgo-Sanchez M. Pax2 expression patterns in the developing chick inner ear. Gene Expr Patterns. 2005; 5:763–773. [PubMed: 15979948]

Scott JD, Fischer EH, Demaille JG, Krebs EG. Identification of an inhibitory region of the heat-stable protein inhibitor of the cAMP-dependent protein kinase. Proc Natl Acad Sci U S A. 1985; 82:4379–4383. [PubMed: 2989819]

Shaywitz AJ, Greenberg ME. CREB: a stimulus-induced transcription factor activated by a diverse array of extracellular signals. Annu Rev Biochem. 1999; 68:821–861. [PubMed: 10872467]

Stamataki D, Ulloa F, Tsoni SV, Mynett A, Briscoe J. A gradient of Gli activity mediates graded Sonic Hedgehog signaling in the neural tube. Genes Dev. 2005; 19:626–641. [PubMed: 15741323]

Tiecke E, Turner R, Sanz-Ezquerro JJ, Warner A, Tickle C. Manipulations of PKA in chick limb development reveal roles in digit patterning including a positive role in Sonic Hedgehog signaling. Dev Biol. 2007; 305:312–324. [PubMed: 17376427]

Trousse F, Marti E, Gruss P, Torres M, Bovolenta P. Control of retinal ganglion cell axon growth: a new role for Sonic hedgehog. Development. 2001; 128:3927–3936. [PubMed: 11641217]

Tuson M, He M, Anderson KV. Protein kinase A acts at the basal body of the primary cilium to prevent Gli2 activation and ventralization of the mouse neural tube. Development. 2011; 138:4921–4930. [PubMed: 22007132]

Wang B, Fallon JF, Beachy PA. Hedgehog-regulated processing of Gli3 produces an anterior/posterior repressor gradient in the developing vertebrate limb. Cell. 2000; 100:423–434. [PubMed: 10693759]

Wang W, Grimmer JF, Van De Water TR, Lufkin T. Hmx2 and Hmx3 homeobox genes direct development of the murine inner ear and hypothalamus and can be functionally replaced by Drosophila Hmx. Developmental cell. 2004; 7:439–453. [PubMed: 15363417]

Wang W, Van De Water T, Lufkin T. Inner ear and maternal reproductive defects in mice lacking the Hmx3 homeobox gene. Development. 1998; 125:621–634. [PubMed: 9435283]

Wen W, Harootunian AT, Adams SR, Feramisco J, Tsien RY, Meinkoth JL, Taylor SS. Heat-stable inhibitors of cAMP-dependent protein kinase carry a nuclear export signal. J Biol Chem. 1994; 269:32214–32220. [PubMed: 7798221]

Wen W, Meinkoth JL, Tsien RY, Taylor SS. Identification of a signal for rapid export of proteins from the nucleus. Cell. 1995; 82:463–473. [PubMed: 7634336]

Wu DK, Kelley MW. Molecular mechanisms of inner ear development. Cold Spring Harb Perspect Biol. 2012; 4:a008409. [PubMed: 22855724]

Highlights

1. PKA activity forms a dorsal-high to ventral-low gradient across the otocyst.
2. The ventral otocyst, which receives high SHH signaling, has low PKA activity.
3. Low PKA activity suppresses GLI3 processing, leading to a low GLI3R/FL ratio.
4. The low GLI3R/FL ratio regulates gene expression, establishing ventral polarity.

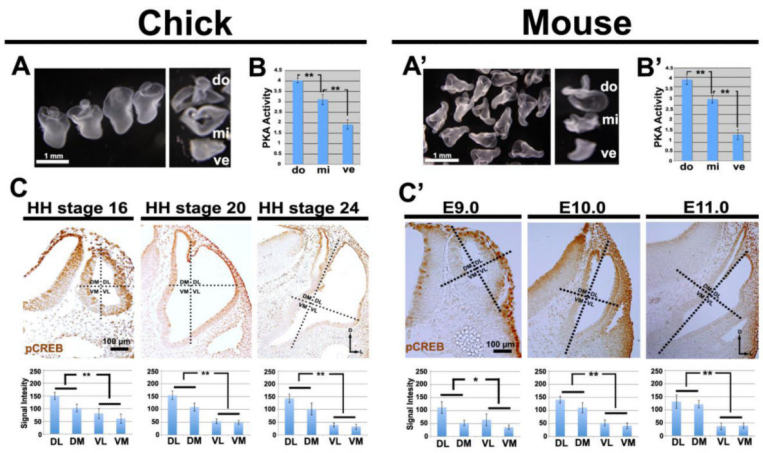

Figure 1. PKA activity and pCREB labeling form dorsal-high to ventral-low gradients in chick and mouse otocysts

(A, A') Collection of chick (HH stage 24) and mouse (E10.5-E11.0) otocyst dorsal (do), middle (mi), and ventral (ve) fragments to assess PKA activity. **(B, B')** Graphs showing the mean levels of PKA activity assayed in the three groups of pooled fragments in each organism (unit: pmol ATP/min/μg protein). n=9 chick PKA assays; n=4 mouse PKA assays. **(C, C')** pCREB labeling in sections of chick (HH stages 16, 20, and 24) and mouse (E9.0, E10.0, and E11.0) otocysts, and graphs showing mean levels of pCREB signal intensity (unit: 8-bit gray scale value; minimum: 0, maximum: 255). Chick: n=5 embryos at HH stage 16, n=9 embryos at HH stage 20, n=12 embryos at HH stage 24; mouse: n=5 embryos for each of the three stages. Dotted lines indicate the subdivision of the otocyst into quadrants (DM, dorsomedial; DL, dorsolateral; VM, ventromedial; VL, ventrolateral) used for quantification. Abbreviations here and in subsequent figures: *, $P<0.05$; **, $P<0.01$; D, dorsal; L, lateral.

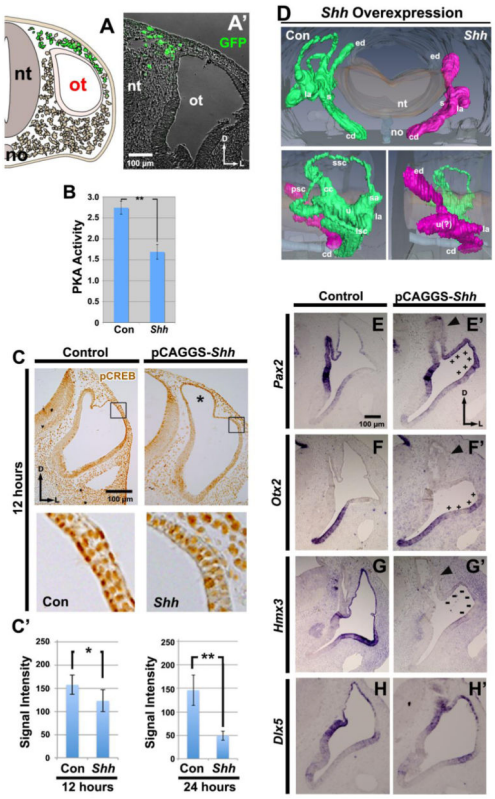

Figure 2. *Shh* overexpression in dorsal head mesenchyme inhibits PKA activity and CREB phosphorylation, ventralizing the otocyst

(A) Scheme showing targeting of dorsal head mesenchyme by sonoporation with *Shh* and *Gfp* vectors and (**A'**) a transverse section 12 hours after transfection with *Gfp*. Abbreviations here and in subsequent figures: nt, neural tube; no, notochord; ot, otocyst. Transfected cells are shown in green. **(B)** Graph showing the mean level of PKA activity (unit: pmol ATP/min/μg protein) assayed in pooled whole otocysts collected 24 hours after overexpression of *Shh* and compared with otocysts on the non-transfected side of each embryo (here and in subsequent figures: Con, control). n=6 PKA assays. **(C)** Detection of pCREB in sections of chick otocysts collected 12 hours after *Shh* overexpression (unit: 8-bit gray scale value; minimum: 0, maximum: 255). Boxes show regions enlarged below. Graphs show the mean level of PKA activity at 12 and 24 hours after *Shh* overexpression. 12 hours: n=8 for both control and experimental embryos; 24 hours: n=8 for both control and experimental embryos. Asterisk, enlarged endolymphatic duct. **(D)** Reconstruction of serial sections of chick inner ears collected 5-6 days after *Shh* overexpression. Frontal (top single panel) and lateral (bottom paired panels) views are shown. n=7 embryos sectioned; n=1 embryo reconstructed. **(E-H)** ISH of sections of chick otocysts collected 36 hours after *Shh* overexpression showing the expression patterns of *Pax2*, *Otx2*, *Hmx3* (n=5 for both control and experimental embryos for each gene), and *Dlx5* (n=3 for both control and experimental embryos). Plus signs indicate ectopic expression; minus signs indication loss of expression. Arrowsheads, seemingly dying cells in the endodolymphatic duct. Abbreviations here and in subsequent figures: ed, endolymphatic duct; la, lateral ampulla; s, saccule; cd, cochlear duct;

ssc, superior semicircular canal; sa superior ampulla; psc, posterior semicircular canal; cc, common crus; u, utricle; la lateral ampulla; lsc, lateral semicircular canal.

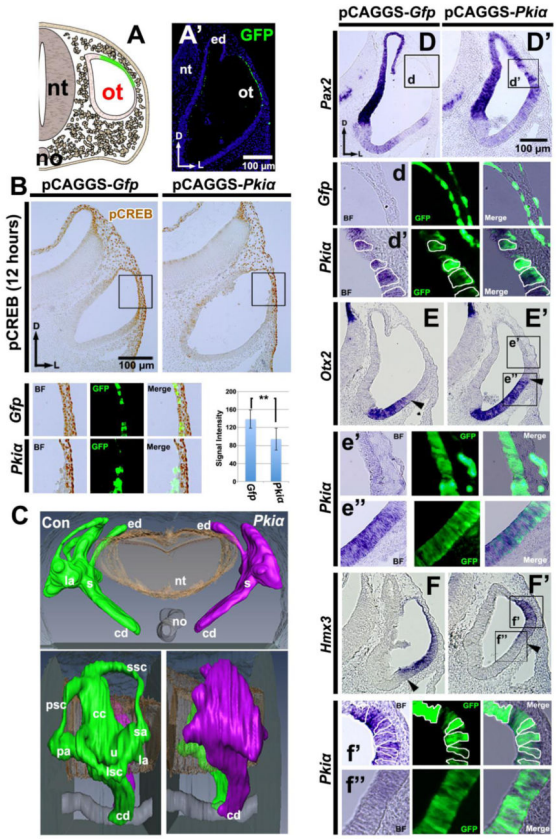

Figure 3. *Pkiα* overexpression in the dorsolateral otocyst also ventralizes the otocyst

(A) Scheme showing targeting of the dorsolateral wall of the otocyst by electroporation of *Pkiα* and *Gfp* and (**A'**) a transverse section 12 hours after transfection with *Gfp*. **(B)** Detection of pCREB in sections of chick otocysts collected 12 hours after overexpression of *Gfp* alone, or of *Pkiα* and *Gfp*. n=11 embryos analyzed for both controls and experimentals. Boxes show regions enlarged below. Graph shows the mean value of pCREB signal intensity (unit: 8-bit gray scale value; minimum: 0, maximum: 255) that was assessed specifically in transfected (GFP positive) cells. **(C)** Reconstruction of serial sections of chick inner ears collected 5-6 days after *Pkiα* overexpression. Frontal (top single panel) and lateral (bottom paired panels) are shown. n=6 embryos sectioned; n=1 embryo reconstructed. (**D-F**) ISH of sections of chick otocysts collected 12-16 hours after *Pkiα* overexpression showing *Pax2*, *Otx2*, and *Hmx3* expression. n=6 for both control and experimental embryos for each gene. Boxes show regions enlarged below, with borders of selected cells outlined. Arrowheads indicate the boundary of the dorsal *Otx2*- and ventral *Hmx3*-expression domains.

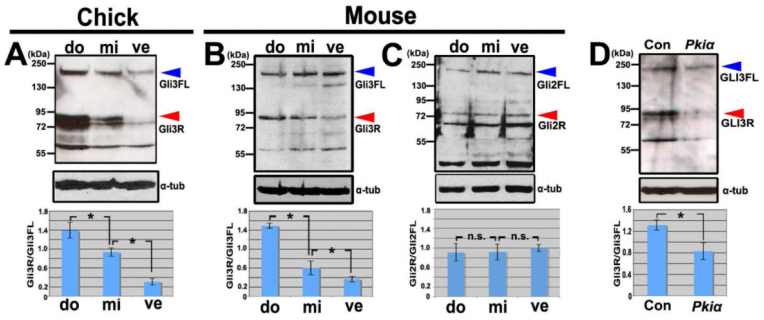

Figure 4. The ratio of GLI3 repressor to GLI3 full-length forms dorsal-high to ventral-low gradients in chick and mouse otocysts

(A) Western blot and graph showing the ratios of GLI3R to GLI3FL in the three groups of pooled chick otocyst fragments (shown in Fig. 1A). n=3 western blots. **(B)** Western blot and graph showing the ratios of GLI3R to GLI3FL in the three groups of pooled mouse otocyst fragments (shown in Fig. 1A'). n=4 western blots. **(C)** Western blot and graph showing the ratios of GLI2R to GLI2FL in the three groups of pooled mouse otocyst fragments (shown in Fig. 1A'). n.s., not statistically significant. n=3 western blots. **(D)** Western blot and graph showing the ratios of GLI3R to GLI3FL in whole chick otocysts 12-16 hours after overexpression (as shown in Fig. 3A) of *Gfp* alone, or of *Pkiα* and *Gfp*. n=7 western blots. Red arrowheads indicate the GLI3R band at 83kDa and blue arrowheads indicate the GLI3FL band at 190kDa. α-tub, α-tubulin.

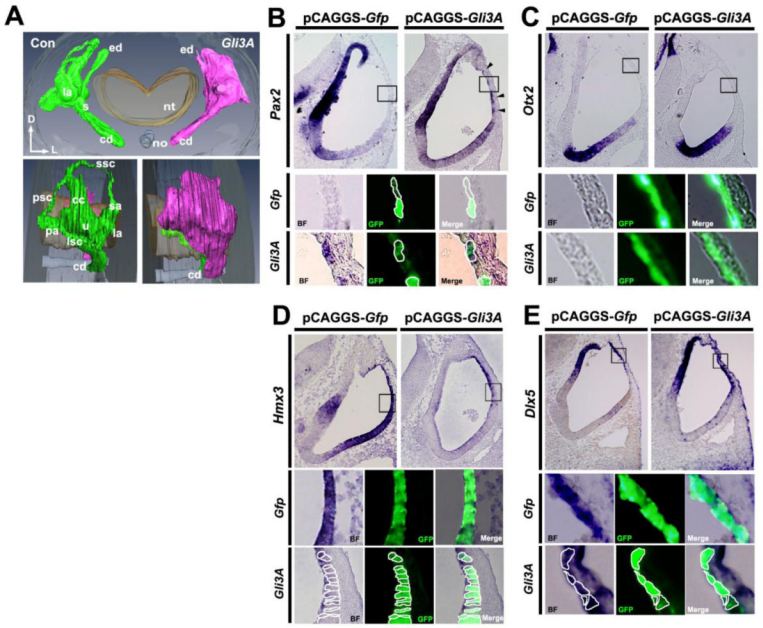

Figure 5. Altering the GLI3R/GLI3FL ratio by overexpressing *Gli3A* in the dorsolateral otocyst perturbs DV polarity of the otocyst

(A) Reconstruction of serial section of chick inner ears collected 5-6 days after *Gli3A* overexpression (as shown in Fig. 3A). Frontal (top single panel) and lateral (bottom paired panels) are shown. n=5 embryos sectioned; n=1 embryo reconstructed. **(B-E)** ISH of sections of chick otocysts collected 12-16 hours after overexpression of *Gfp* alone or *Gli3A* and *Gfp* showing *Pax2*, *Otx2*, *Hmx3*, and *Dlx5* expression. For *Otx2*: n=3 for both control and experimental embryos; for *Pax2*, *Hmx3*, and *Dlx5*: n=4 for both control and experimental embryos. Boxes show regions enlarged below, with borders of selected cells outlined. Arrowheads in **B** indicate dorsal otocyst cells ectopically expressing *Pax2*.

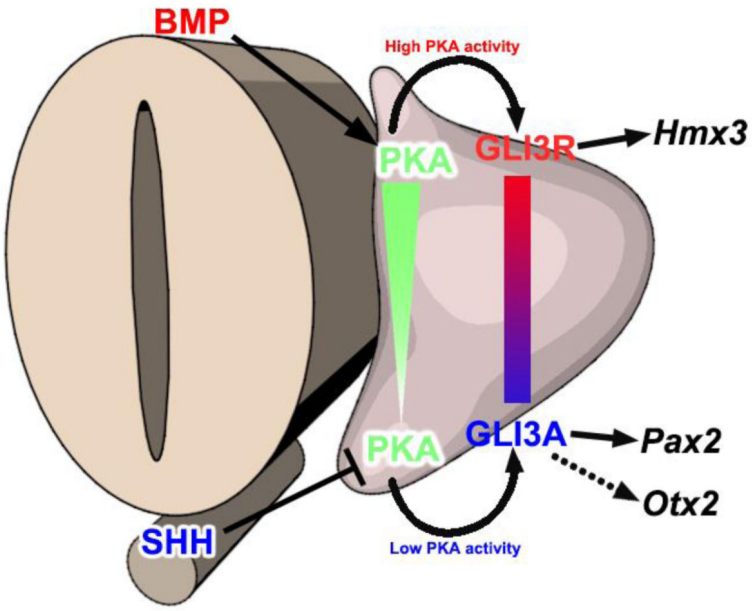

Figure 6. Model: PKA activity is a common intersection point coordinating dorsalizing and ventralizing signals in the early otocyst

SHH signaling emanating from the floor plate of the neural tube and notochord maintains low PKA activity in the ventral otocyst, whereas BMP signaling in the dorsal otocyst activates PKA; thus, a gradient of PKA activity forms across the DV axis of the otocyst. High PKA activity in the dorsal otocyst results in high GLI3FL partial proteolytic processing, the accumulation of GLI3R, and the expression of *Hmx3*. In contrast, low PKA activity in the ventral otocyst results in low GLI3FL proteolytic processing, the maintenance of GLI3FL (potentially GLI3 activator), and the expression of *Pax2* and *Otx2*.